




# Favorable formation of stereocomplex crystals in long-chain branched poly(L-lactic acid)/poly(D-lactic acid) blends: impacts of melt effect and molecular chain structure

Zhongguo Zhao<sup>1</sup>, Dahang Tang<sup>2,\*</sup> , Shikui Jia<sup>1</sup>, and Taotao Ai<sup>1,\*</sup>

<sup>1</sup>National and Local Engineering Laboratory for Slag Comprehensive Utilization and Environment Technology, School of Materials Science and Engineering, Shaanxi University of Technology, Hanzhong 723000, China

<sup>2</sup>Centre for Polymer and Material Technologies, Department of Materials, Textiles and Chemical Engineering, Ghent University, Technologiepark 130, 9052 Zwijnaarde, Belgium

Received: 29 August 2020

Accepted: 16 December 2020

Published online:

3 January 2021

© The Author(s), under exclusive licence to Springer Science+Business Media, LLC part of Springer Nature 2021

## ABSTRACT

A feasible approach is proposed to promote the formation of the stereocomplex crystal ( $S_c$ ) in long-chain branched Poly(L-lactic acid)/Poly(D-lactic acid) (LCBPLA/PDLA) blends with hydrogen bond interactions. The synergistic effect of PDLA and long-chain branches significantly increases the crystalline ability of  $S_c$  from 20.1 to 30.4% due to the improved intermolecular crystal nucleation/growth. The frequency-independent loss tangent appeared at a PDLA concentration of 5.0 wt%, indicating a transition from the liquid-like to solid-like viscoelastic and the formation of a network composed of long-chain branches and the reserved  $S_c$  crystallites. Changing the processing temperatures from 190 to 230 °C seems to induce different melting behavior of  $S_c$  with diverse topological conformations so as to act as a template to attract PLLA molecule chains to perform the crystallization behavior. In situ wide-angle X-ray diffraction analysis reveals that a higher cooling temperature (less than 220 °C) significantly contributes to the  $S_c$  with more integrated structures and the  $H_c$ -to- $S_c$  transition. The polarizing optical microscope results show that increasing the PDLA content and long-chain branched points significantly promote the spherulite growth and nuclei density of  $S_c$ , increasing the  $S_c$  size from 56.47 to 94.13  $\mu\text{m}$  and nuclei density from 52.2 to 98.3%.

Handling Editor: Gregory Rutledge.

Address correspondence to E-mail: tangdahang0908@126.com; aitaotao0116@126.com

## Introduction

The energy shortage and environmental pollution problems are big issues in modern society, which are the major concerns for a sustainable development with aspect to industrial applications and economics [1, 2]. The bio-based polymers such as poly (L-lactic acid) (PLLA) are attracting a lot of attentions in recent years due to their good biodegradability, excellent mechanical properties and renewability [3–5]. However, their low melt strength at least caused by the crystallization ability limits their applications in view of the industrial aspects to some extent. To address these issues, modifications of the general linear PLA material by means of introducing the nucleating agent, inorganic particle and even changing its molecular structures are taken into consideration in literature work [6, 7]. Apart from these methods, an in situ formation of the stereocomplex crystallites ( $S_c$ ) has also been proved to an effective and promising method and strategy to improve the thermal stability and crystallization ability [8–10].

In the past twenty years, great efforts have been carried out to investigate the mechanism and thus the possible factors efficiently affecting the formation of  $S_c$ . For example, it is reported that the component ratio of 50/50 for PLLA/PDLA blend can generally achieve a complete  $S_c$  formation, while many factors including molecular weight (MW), processing temperatures and blending ratio et al. have a significant impact on the relative content of  $S_c$  [11–17]. In addition, Pan et al. [18] investigated the competitive behavior between the forming of homocrystallization ( $H_c$ ) and  $S_c$  in PLLA/PDLA racemic blends and revealed that increasing the molecular weight of PLLA sharply depressed the latter behavior. For example, for PLLA/PDLA blends with medium (MW > ~ 40 kDa) and high MWs (MW > ~ 80 kDa),  $H_c$  crystallization becomes predominant in comparison with  $S_c$  crystallization behavior during the conventional processing conditions [19]. As a result, the critical issue comes into mind that how to improve the formation of  $S_c$  but suppress that of  $H_c$  correspondingly in terms of the practical processing. It is expected that high-molecular-weight (HMW) PLLA/PDLA blends should have a rather complicated crystallization ability, thus resulting in various crystalline structures, however, the underlying mechanism still remains indistinct.

Researchers have put forwards the importance of the investigation on the effect of molecular structures on the nucleation mechanism and crystal growth of  $S_c$  based on the HMW PLLA-based material with various molecular architectures [14, 20, 21]. For instance, Brochu et al. [20] studied the forming mechanism of the  $S_c$  for asymmetric PLLA/PDLA blends and proved that only adding 10 wt % PDLA was able to accelerate the formation of  $S_c$ . Biela et al. [15] reported that the change of molecular structure can influence the formation of  $S_c$ , in which the obtained perfect  $S_c$  crystallites are stemming from the star-shaped HMW PLLA with six arms or more. Recently, Bao et al. [21] showed that a lower processing temperature of 160 °C contributed to the complete stereocomplex crystallites without homocrystallites for high-molecular-weight PLLA/PDLA blends. In addition, in our previous report [2], we successfully prepared the HMW PLLA material with long-chain branches, which played a role in significantly improving the crystalline properties. Overall, although the studies regarding the crystallization behavior of PLLA have been carried out in large amounts [22–26], based on the knowledge of the authors, few reports have concentrated on the effect of processing condition like the melting temperature and branched molecular structure on the crystallization behavior and polymorphism of the long-chain branched PLLA/PDLA blend. However, this potentially provides guidance for promoting the industrial application of PLA-based materials.

In this work, a simple and effective method for enhancing the contents of  $S_c$  crystals in LCBPLA/PDLA blends was proposed. The effects of melt memory effect or the so-called template effect and molecular structure on the crystalline kinetic, polymorphic crystalline structure and structural reorganization were comprehensively investigated by these DSC, in situ WAXD, rotational rheometer and POM characterizations. Emphasis is paid on the factors of melting temperatures and long-chain branches of polymer blends, the interplays of which complicatedly influence the relative content of  $S_c$  crystals of these PLLA blends. In addition, the mechanism for enhancing the stereocomplex ability of LCBPLA/PDLA blends was also discussed and proposed.

## Materials and methods

### Materials

Poly (L-lactic acid) (PLLA, 4032D, NatureWorks and  $M_w \approx 10^6$  g/mol) comprising around 2% D-LA was used in this study. The optical purity and  $M_w$  of PDLA are about > 98% and 141 kg/mol, respectively. PLLA and PDLA pellets were dried at 60 °C for 24 h under vacuum condition before mixing. Pentaerythritol triacrylate (PETA), Dicumyl peroxide (DCP) and Tetraethyl thiuram disulfide (TETDS) were all bought from the Sigma company and used as received.

### Sample preparation

The long-chain branched PLLA (LCBPLA) was prepared and the long-chain branched structure (as shown in Fig. 1) can be obtained according to our previous report [2]. Briefly, the monomer PETA and DCP were used to modify the linear PLLA. Then, the dried obtained PLLA + 0.4%PETA (denoted as LCBPLA in next section) pellets were chosen to blend with different contents of PDLA in the dichloroethane solvent. The corresponding detailed formulation of each sample is listed in Table 1.

### Measurements

#### Differential Scanning Calorimetry (DSC)

All the samples with a mass of around 5 ~ 8 mg were heated from 40 to 240 °C to investigate the melting behavior using the TA Instruments DSC Q20 under nitrogen atmosphere condition with a heating rate of 10 °C/min. As for the nonisothermal

crystallization, the samples with 5 ~ 8 mg were firstly heated from 40 °C to the treatment temperatures ( $T_s = 190 \sim 230$  °C) at a heating rate of 10 °C/min, and stayed at this temperature for 5 min to eliminate the heat history. And then the samples were cooled down to 40 °C at a cooling rate of 3 °C/min.

#### In situ WAXD measurements

Synchrotron two-dimensional wide-angle X-ray diffraction (2D-WAXD) experiments were performed at BL16B1 of Shanghai Synchrotron Radiation Facility (SSRF, Shanghai, China) to investigate the crystallization behavior. The Linkam THMS-600 hot stage was used to precisely control the experiment temperature. To observe the changes of crystalline structures, the sample was heated from 40 °C to a certain temperature ( $T_s = 190, 220$  and 230 °C) with a heating rate of 30 °C/min. After that, the sample was cooled down to 80 °C with a cooling rate of 3 °C/min. During cooling stage, the data were on-line recorded by the MAR CCD detector (MAR-USA).

#### Rheological measurement

A strain-controlled rotational rheometer (ARES, TA instruments, USA) equipped with a 25 mm parallel plate geometry was employed to test the rheological behaviors with the small amplitude oscillatory shear (SAOS) mode. The dynamic frequency sweep was set from 0.1 ~ 1000 rad/s. The rheological samples were prepared using a compression molding with a compression force of 10 MPa at the processing temperature of 180 °C.

#### Polarizing Optical Microscope (POM)

The nucleation and crystalline morphologies of samples were observed by means of POM (Olympus BX51, Japan) equipped with a hot stage (LINKAM THMS 600). The sample sandwiched between two cover glasses was fully melted at 230 °C for 5 min. And then, the sample was quickly cooled down to a certain temperature of 156 °C with a cooling rate of 30 °C/min and then stayed for 40 min for an isothermal crystallization. During this process, the data were on-line recorded automatically.

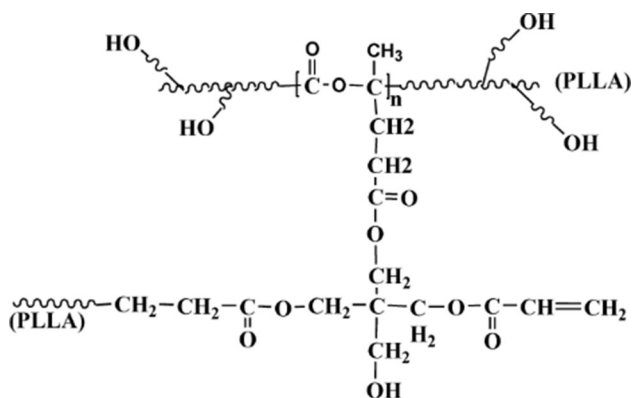


**Figure 1** Structural formula of LCBPLA.

**Table 1** The formulations and abbreviations of samples

Samples	PLLA(g)	DCP(g)	TETDS(g)	PETA(g)	PDLA(wt%)	PDLA(g)
Pure PLLA	65	–	–	–	–	–
PLLA + 10%PDLA	58.5	–	–	–	10	6.5
LCBPLA	65	0.04	0.18	0.26	0	0
LCBPLA + 1%PDLA	64.4	0.04	0.18	0.26	1	0.65
LCBPLA + 3%PDLA	62.6	0.04	0.18	0.26	3	1.95
LCBPLA + 5%PDLA	61.3	0.04	0.18	0.26	5	3.25
LCBPLA + 8%PDLA	58.7	0.04	0.18	0.26	8	5.2
LCBPLA + 10%PDLA	58.0	0.04	0.18	0.26	10	6.5

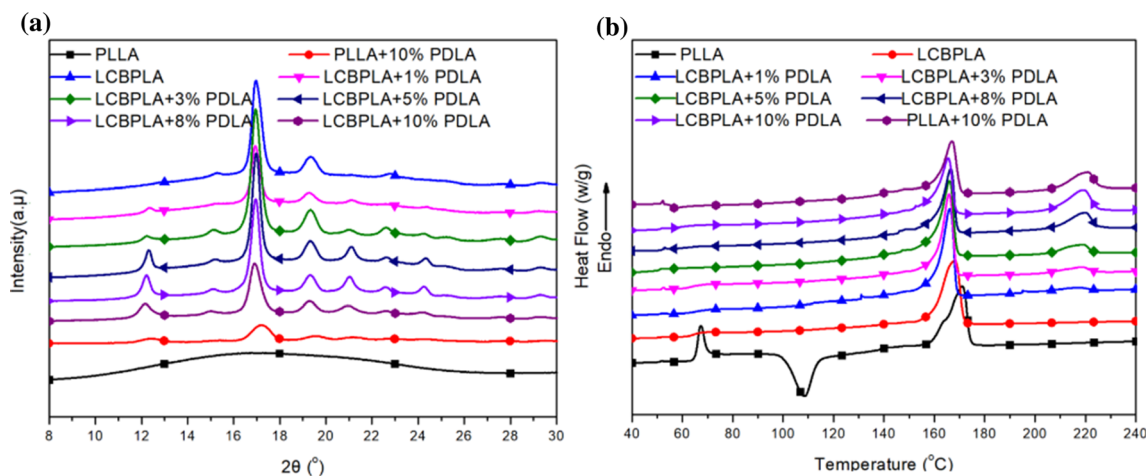
## Results and discussion

### Relation between the long-chain branches and effect on crystallizations

The formation of  $S_c$  in PLLA/PDLA blends with different contents of PDLA prepared by solution casting (25 °C) method was investigated by WAXD and DSC. As shown in Fig. 2, in comparison with the pure PLLA material, the diffraction peak at the diffraction degree of 12.1, 21.2, and 24.1° with adding PDLA indicates the formation of PLLA stereocomplex crystallites ( $S_c$ ) [27]. Furthermore, a further increasing the PDLA content from 1 to 10 wt% obviously strengthens the diffraction intensity of  $S_c$  crystals of LCBPLA blends. Compared with LCBPLA/PDLA blends, a weak but still visible diffraction peak at 12.1° appears for the liner PLLA/PDLA blend, corresponding to the  $S_c$  crystallites. It is ascribed to the reason that the liner PLLA has a much lower crystallinity and crystallization ability to form  $S_c$ . In contrast, it should be noted that the addition of

PDLA into the long-chain branched blends can promote the polymorphism with multiplied diffraction peaks.

It is seen in Fig. 2b that only a single peak at around 165 °C can be discerned for PLLA and LCBPLA samples, indicating the complete homocrystallites ( $H_c$ ) structures without a companying of the  $S_c$ . However, regarding other samples blended with PDLA, there is another obvious melting peak at ~ 220 °C shown on the DSC curves, which again proves the existence of the crystalline structure ( $S_c$ ). In contrast to the pure PLLA samples, the formation of stereocomplex crystals in the series of the PLLA + 10% PDLA samples significantly improves the crystalline behavior and thus contributes to a higher crystallinity degree during the practical processing. As a result, the cold crystalline peak of PLLA material vanishes for all PLLA blends with adding PDLA. In addition, it is observed that increasing the content of PDLA slightly raises the melting temperature of stereocomplex crystallites ( $T_{m,sc}$ ) from 217.2 to 220.5 °C but decreases the melting temperature of

**Figure 2** WAXD **a** and DSC melting **b** profiles of the compression-molded samples.

homocrystallites from 167.1 °C to 162.8 °C for LCBPLA composites as compared. Overall, it seems that increasing the PDLA content facilitates the stereocomplex crystal with more integrated structures or thicker lamellas.

To quantitatively compare the content of  $S_c$  component in all the crystals formed during the processing, the relative fraction of  $S_c$  ( $f_{S_c, DSC}$ ) in the crystalline phase of samples was estimated with the DSC data by a term  $f_{S_c}$ , which is defined as  $f_{S_c} = 100\% \times X_{S_c} / (X_{S_c} + X_{H_c})$ . The corresponding calculated results were displayed in Table 2. It is worth to mention that a large value range of  $f_{S_c}$  from 0 to 20% can be achieved by only adjusting the PDLA content added in the PLA blends. In addition, within a same content of 10 wt% PDLA, introducing the long-chain branches onto the molecular structures of PLA material leads to an increase of the crystallinity of  $S_c$  from 11.2 to 13.5% and decrease of crystallinity of  $H_c$ , thus resulting in a higher relative content value of  $S_c$  ( $f_{S_c}$ ) increases from 20 to 30% as well, as compared to its linear counterpart. Therefore, it is concluded that the LCBPLA chain promotes the increase of  $S_c$  in blends and the reasons are shown as follows: intermolecular crystal nucleation and growth are crucial factors for the development of crystalline structures. Firstly, although forming the long-chain branches can restrain the diffusion and mobility of the bridged and surrounded chains, more nucleation sites are obtained due to the more branched structures of the long-chain branched blends compared with liner PLLA chains. Once the melt is cooled down, the  $S_c$  crystals can firstly be formed, leading to the formation of three-dimensional physically cross-linked networks [28–30]. It is attributed to smaller kinetic energy barrier of  $S_c$  crystals than that of  $H_c$ ,

even though the latter seems to be more thermodynamically favorable. Secondly, LCBPLLA/PDLA blends own more intermolecular H-bond interactions between enantiomers may favor the intermolecular crystal nucleation and growth, resulting in the enhanced  $S_c$ .

To have a direct insight into the difference of  $S_c$  crystallite caused by factors of the PDAL and long-chain branches introduced into the PLLA blends, we delicately designed a dissolution experiment to reveal the formed networks of molecular configurations of the blends. It is noted in Fig. 3 that both pure PLLA and LCBPLA are expected to be completely dissolved in the dichloromethane solvent with a complete transparency, indicating the long-chain branches are not able to prevent the PLLA chains from being dissolved in the dichloromethane solvent. Once PDLA was added into the PLLA blend, it is found that some undissolved white particles suspended in the solution, which is ascribed to the  $S_c$  crystallite which has a trend in remaining its original configurations in the presence of the dichloromethane solvent in Fig. 3c–e. Increasing the PDLA content from 3 wt% to 10 wt% seems to clearly result in larger white suspended particles. Furthermore, in Fig. 3d, the long-chain branches attached to the linear PLLA molecules are in favor of larger white particles as compared to the completely linear PLLA material blended with the same content of 10 wt% PDLA, indicating larger amount of  $S_c$  crystallites for LCBPLA blend as well, which is in consistent with the results shown in Fig. 2. It should be noted that  $S_c$  are thought to act as likely the physical ‘cross-linking’ points for these PLLA chains, the schematic image of which is shown in Fig. 3d, e. Due to the existence of the cross-linked structures, this makes these interactional PLLA molecule chains relax in a much slower

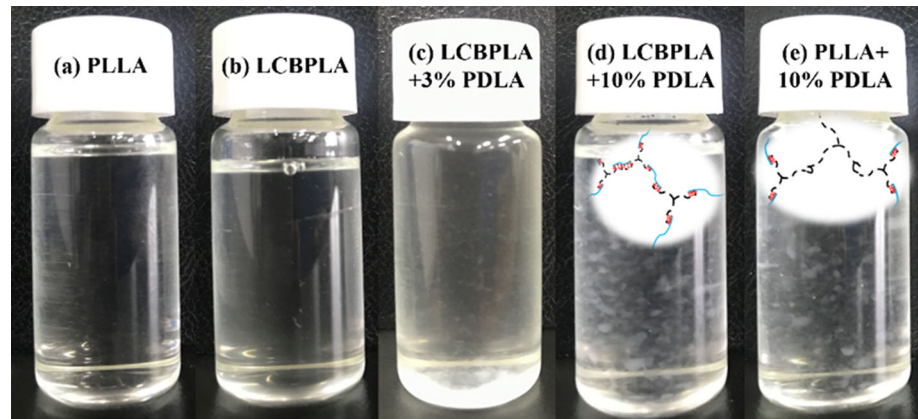
**Table 2** Crystalline information of  $H_c$  and  $S_c$  in Samples

Sample	$T_{m, H_c}$ (°C)	$T_{m, S_c}$ (°C)	$X_{S_c}$ (%)	$f_{S_c}$ (%)
PLLA	168.6	–	0	0
PLLA + 10%PDLA	166.9	220.5	11.1	20.1
LCBPLA	167.1	–	0	0
LCBPLA + 1%PDLA	167.2	217.2	1.1	2.3
LCBPLA + 3%PDLA	165.6	218.1	4.3	9.4
LCBPLA + 5%PDLA	166.4	218.9	5	11.2
LCBPLA + 8%PDLA	163.1	220.2	8.8	18.3
LCBPLA + 10%PDLA	162.8	220.5	13.5	30.4

Relative content of  $S_c$  is calculated as  $f_{S_c} = \frac{X_{S_c}}{X_{S_c} + X_{H_c}} \times 100\%$



**Figure 3** The pictures of the dissolved samples in dichloromethane which were taken after the solutions were remained for 24 h.



way and tend to take part in the formation of configuration networks composed of  $S_c$  crystals and molecule chains. Therefore, it accounts for the undissolved white suspended particles in the dichloromethane solvent in Fig. 3. Overall, it confirms again that both increasing PDLA content and introducing the long-chain branches promote the development of  $S_c$  during the practical processing.

### The effect of long-chain branches and crystalline structure on the rheological behavior

Rheological test can be an effective and meaningful tool to probe the network structures of materials with the rheological functions such as storage modulus  $G'(\omega)$  and loss modulus  $G''(\omega)$  by means of the small amplitude oscillatory shear (SAOS) measurement. Figure 4 shows the rheological properties for various PLLA blends at 180 °C, at which only the homocrystallites of the PLLA material are melted while the  $S_c$  crystallites remain their solid phase with a high melting point of 220 °C, looking back to Fig. 2b.

In Fig. 4a, b, neat PLLA chains are fully relaxed and exhibited the typical terminal behavior with the scaling law of approximate  $G' \propto \omega^2$  and  $G'' \propto \omega^1$ . Introducing the PDLA into PLLA or LCBPLA can significantly increase the  $G'$  and  $G''$  values. As for the LCBPLA/PDLA blends, increasing the PDLA content tremendously enhances the  $G'$  and  $G''$  values, especially at the low frequency range. A relatively larger change of the  $G'$  compared to that of  $G''$  for the long-chain branched samples implies that the elastic properties of PLLA chains are more sensitive to the  $S_c$  crystals. Furthermore, increasing the PDLA content

from 3 wt% to 10 wt% can decrease the slope of the modulus curves, indicating that the relaxation behavior of blends becomes slow. This phenomenon may be ascribed to the network structures of  $S_c$  which restrains the long-range motions of polymer chains [31, 32]. Moreover, it is presented that adding the long-chain branches into PLLA + 10%PDLA blends further increases the  $G'$ , resulting from more integrated network structures composed of long-chain branches and  $S_c$  crystals.

The loss tangent ( $\tan\theta = G'/G''$ ) is thought to be more sensitive and meaningful to the molecular relaxation behavior than  $G'$  and  $G''$  [33]. The  $\tan\theta$  of pure PLLA is remarkably decreased with the increasing  $\omega$ , verifying that the typical character of PLLA material as a viscoelastic liquid. However, as for other samples, increasing  $\omega$  can gradually decrease  $\tan\theta$ , which reflects that the elastic behavior becomes dominating [34]. This phenomenon becomes more distinct with the increase of PDLA concentration, stemming from the formation of  $S_c$  network. Therefore, we define the amount of 5 wt% as the critical value for the formation of a network composed of long-chain branches and the reserved  $S_c$  crystallites, which is consistent with the results reported by Winter et al. [35, 36]. In addition, the frequency-independent loss tangent also indicates a transition from the liquid-like to solid-like viscoelastic behavior for LCBPLA blends at low frequencies. This demonstrates that the long-range dynamic polymer chains motion is restrained by the formed  $S_c$  crystallite network with polymer molecules significantly, and this restraining effect is even further strengthened by the addition of long-chain branches.

Above all, the rheological results further confirm the existence of the network structures composed of

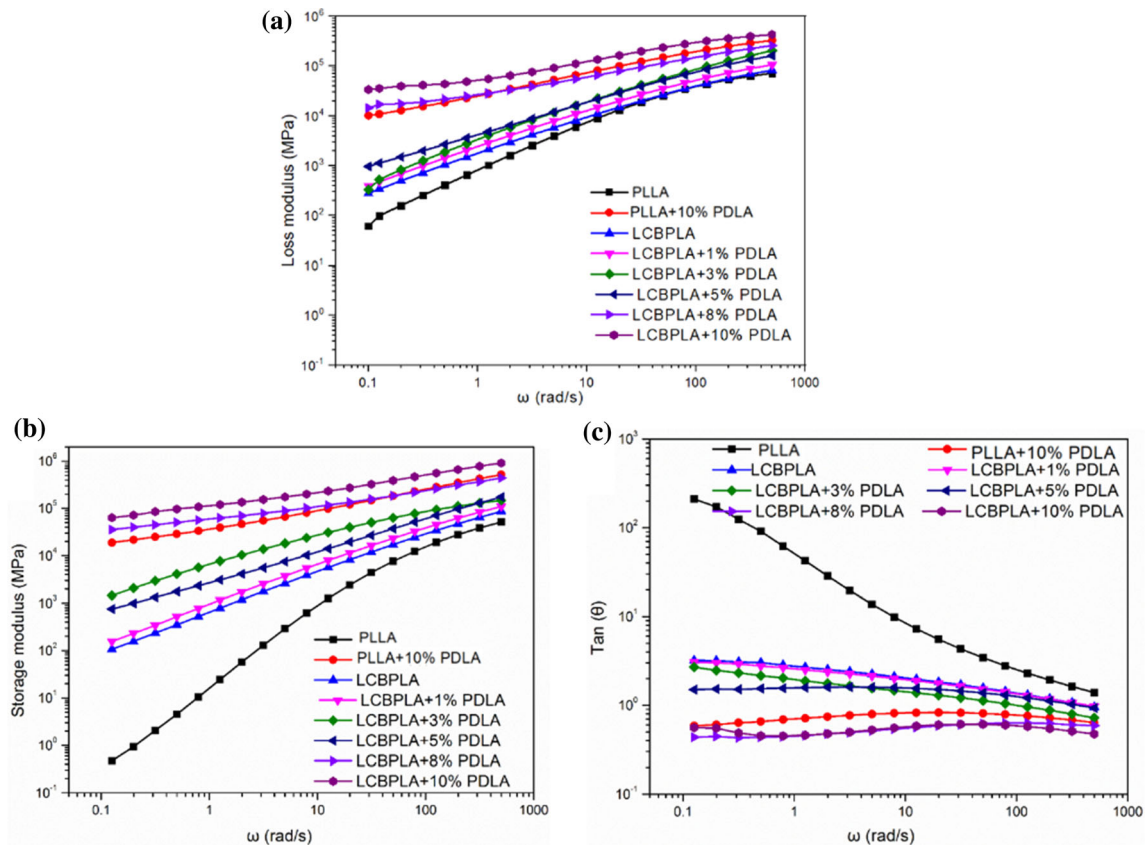


**Figure 4** The changes of **a** storage modulus ( $G'$ ), **b** loss modulus ( $G''$ ) and **c** loss tangent ( $\tan\theta$ ) with frequency dependences ( $\omega$ ) for various PLLA blends.

PLLA chains and  $S_c$  crystals which vary with the content of PDLA and long-chain branches.

### Melting behavior and polymorphic crystalline structure

DSC characterizations were conducted to capture the changes of the melting behavior and polymorphic crystalline structure of the blends as shown in Fig. 5 and Table 3. In Fig. 5a, the crystallization peak of PLLA and PLLA + 10% PDLA samples can be faintly discerned, resulting from the low crystalline ability. However, the formation of  $S_c$  can significantly enhance the onset of the crystalline temperature from 109.6 °C for PLLA to 136.9 °C for PLLA + 10% PDLA. Compared with the pure PLLA sample, the crystalline temperatures (onset of crystalline temperature:  $T_o$  and the peak crystalline temperature:  $T_p$ ) of LCBPLA sample significantly increase due to the formation of long-chain branches, e.g.,  $T_o$  from 109.6 °C for PLLA to 143.4 °C and  $T_p$  from 99.2 °C for PLLA to 139.8 °C, respectively. However, a slight

increase of the LCBPLA blends by mixing with PDLA is achieved, as shown in Fig. 5a. Increasing the PDLA content to 5 wt% results in the highest  $T_o$  and  $T_p$  temperatures with 145.4 and 141.1 °C, respectively. It indicates that the formation of long-chain branches attached to the linear PLLA molecules plays a predominating role in enhancing the crystalline temperatures, although the residual stereocomplex crystals with a higher melting temperature (240 °C) than the melting temperature (200 °C) we choose can contribute to a larger crystallization ability as well.

In addition, an interesting phenomenon was observed in Fig. 5a and Table 3 that introducing the long-chain branches into PLLA blends promotes the crystalline rate of blends, namely the crystallization time decreasing from 6.1 to 2.7 min for liner PLLA. In contrast, the LCBPLA(PLLA)/PDLA blends show an opposite phenomenon, which is accounted for the formation of  $S_c$  decreasing the crystalline rate. This can be ascribed to the formation of structural molecular network between LCBPLA and PDLA shown in Fig. 3, which prohibits the mobility of

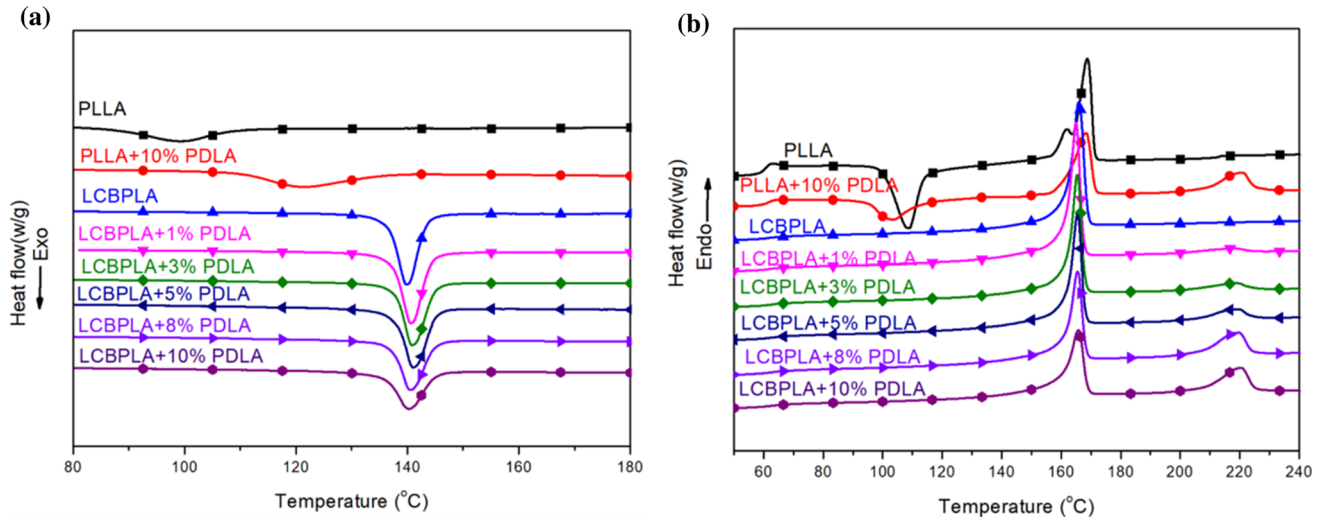


**Figure 5** a DSC cooling curves of samples with the cooling rate and melting temperature being 3 °C/min and 200 °C, respectively; and b the second-melting curves of the same samples and the heating rate is 10 °C/min.

**Table 3** The relative DSC parameters for various PLLA-based blends

Sample	T <sub>o</sub> (°C)	T <sub>p</sub> (°C)	T <sub>0.5</sub> (min)	X <sub>S<sub>c</sub></sub> (%)
PLLA	109.6	99.2	6.1	0
PLLA + 10% PDLA	136.9	121.5	7.9	12.3
LCBPLA	143.4	139.8	2.7	0
LCBPLA + 1%PDLA	144.2	140.1	3.1	1.5
LCBPLA + 3%PDLA	145.1	140.9	3.43	4.1
LCBPLA + 5%PDLA	145.4	141.5	3.35	5.3
LCBPLA + 8%PDLA	144.9	140.6	3.28	9.1
LCBPLA + 10%PDLA	144.8	140.2	2.79	14.2

molecular chains. There are two ways for the polymer crystal nucleation occurring during the nucleation process, including the intramolecular and intermolecular nucleation, respectively. Intramolecular nucleation needs to cross over a lower free energy barrier in contrast to intermolecular nucleation [37, 38]. Hence, the formation of network structures composed of polymer chains and S<sub>c</sub> crystals can simultaneously enhance the density of nucleation and decrease the mobility of molecular chains, inducing the increase of crystalline temperature but decrease the crystallization rate as a consequence. In addition, compared with linear PLA sample and its corresponding blend, the cold crystallization peak of LCBPLA/PDLA blends disappears and the single melting peak instead of the typical double melting peaks becomes sharper in Fig. 5 b. The reason is that the macromolecular chains in the amorphous domains with the improved flexibility and mobility caused by the heating behavior reorganize into the

crystalline regions. Therefore, the cold crystallization peak could reflect the crystallization ability of macromolecular chain segments to a certain degree. The long-chain branches play an important role in forming nucleation sites, markedly enhancing the nucleation ability of PLLA during the cooling process. In our previous report [2], long-chain branches can significantly shift the crystalline temperature to a higher value and enhances the crystalline ability during the cooling process, thus leading to the absence of cold crystalline peak. Interestingly, it should be noted that the crystallinity of S<sub>c</sub> for LCBPLA + 10%PDLA shown in Table 3 has no obvious change compared with that in Fig. 2 and Table 2. It indicates that the S<sub>c</sub> crystals with very highly integrated structures have been formed in the practical processing, which remain stable during the cooling process in Fig. 5. Consequently, it again highlights that the different crystallization behavior of PLLA molecules for PLLA blends as discussed



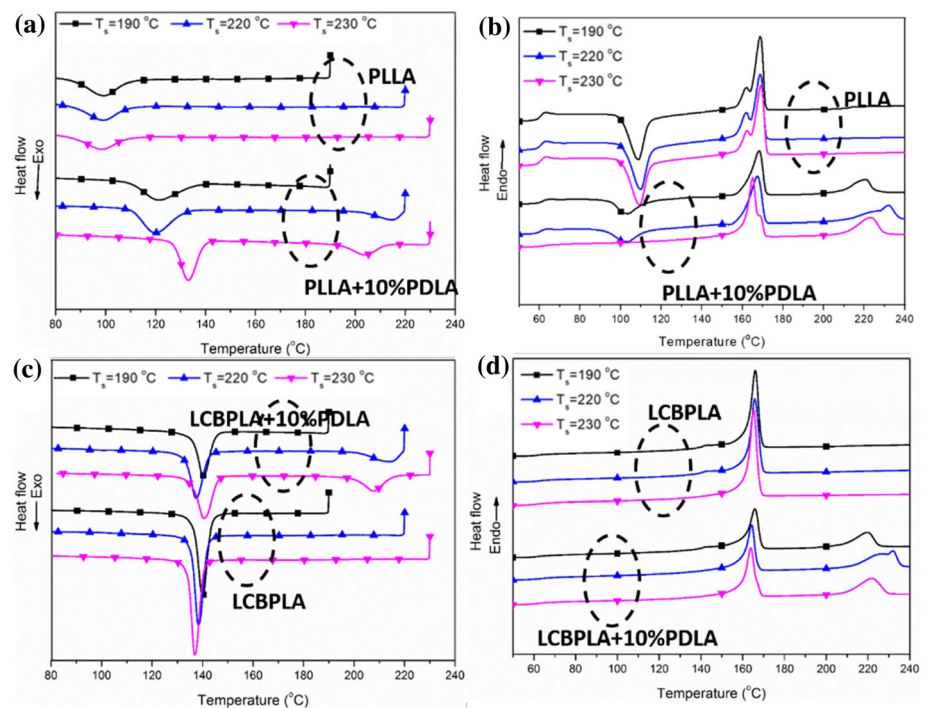
above at least can be attributed to the presence of the residual  $S_c$  crystals. It seems that the residual  $S_c$  crystal served as a preserved template to attract the polymer chains to locate on it, which is defined as kind of ‘memory effect’ for the crystallization behavior of the polymer chains during the second-melting procedure. It on the other hand appears that a programmed crystallization behavior of the PLA chains can be achieved by adjusting this template effect or memory effect caused by the  $S_c$  crystals. This probably enlarges its potential application fields as for this PLLA-based material.

### The melt memory effect on the crystalline structures

With the aim at comprehensively studying the influence on the crystallization behavior of the blends caused by the memory effect and recrystallization of  $S_c$ , the thermal history of the samples during the general processing was investigated, as shown in Fig. 6. It shows the DSC cooling and second-melting curves of the samples at different thermal treatment temperatures ( $T_s$ ). As presented in Fig. 6a, b, the thermal history almost does not influence the crystallization and melting behavior of PLA material, while it leads to a significant effect on that of the PLLA/PDLA blend. For example, increasing the

thermal treatment temperature of PLLA/PDLA blend from 190 to 230 °C firstly decreases the crystallization temperature and then unexpectedly moves that to a higher temperature. This can be attributed to the following two factors. First of all, the uncompleted  $S_c$  crystallites seem to start melting at a higher treatment temperature once the temperature goes lower than the melting point of  $S_c$  crystals ( $T_{m/sc}$  shown in Table 2), which is expected to decrease the number and size of the preformed relatively perfect  $S_c$  crystals. As a consequence, the surface of  $S_c$  is not able to provide enough nucleation sites for the heterogeneous crystallization behavior. However, increasing the treatment temperature ( $\geq T_{m/sc}$ ) allows for promoting the accomplishment of the full melt behavior of the  $S_c$  crystals, which contributes to the release of all the PDLA chains. Secondly, during the cooling stage, the  $S_c$  crystals are thought to recrystallize to act as the templates to attract the molecule chains to reside on them. In addition, the formation of network structure composed of polymer chains and  $S_c$  crystals aforementioned above might take place at a certain temperature between that of  $S_c$  and  $H_c$  crystals, restraining the motions of the molecular chains to some extent. Therefore, when the treatment temperature exceeds the  $T_{m/sc}$  in Fig. 6a, c, the reformed  $S_c$  with a large surface can effectively act as the heterogeneous nucleation sites, increasing the

**Figure 6** The DSC cooling a, c and second-melting b, d curves for different samples such as PLLA with 10 wt% PDLA or not (top images) and LCPLA with 10 wt% PDLA or not (bottom images) at various thermal treatment temperatures.



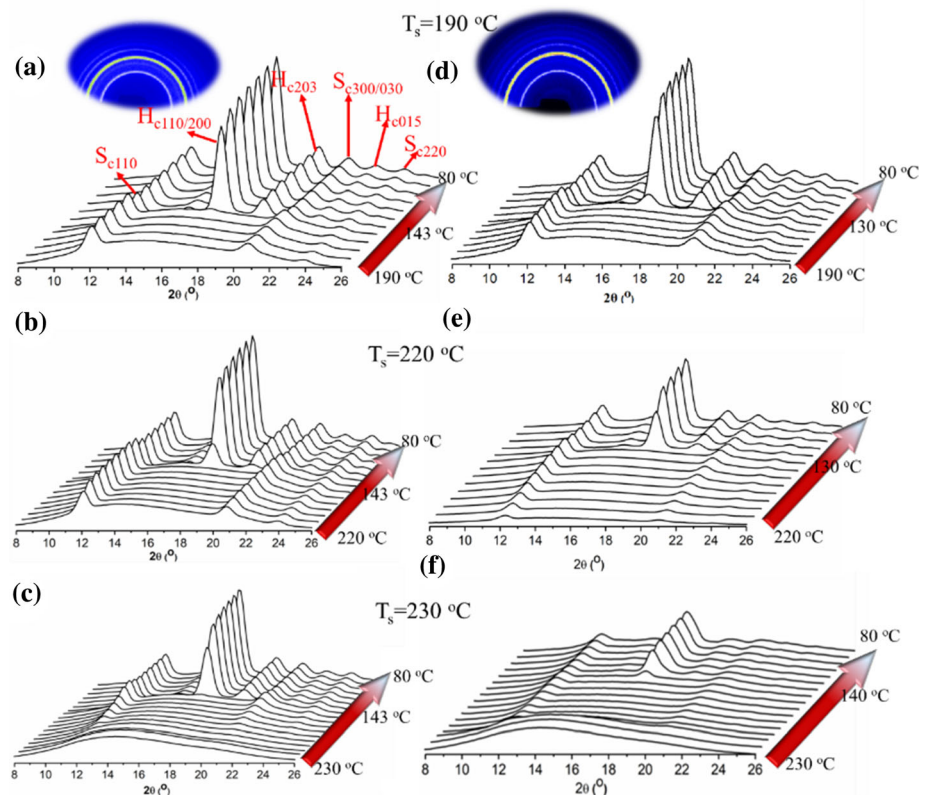
crystallization temperature in return [39]. As shown in Fig. 6b, d, the melting peak of  $H_c$  of PLLA/PDLA blend did not have an obvious change, while the melting temperature of  $S_c$  crystals shifted to a higher temperature when the thermal treatment temperature was below 220 °C. The reason is that the  $S_c$  crystals with less integrated structures seem to melt and recrystallize during this thermal treatment process, leading to the corresponding  $S_c$  crystals with thicker lamellas and more integrated crystalline structures. This similar phenomenon is also observed for LCBPLA blends, as shown in Fig. 6d.

For a further proof and understanding of the crystallization behavior of the blends caused by the formation of  $S_c$  crystals for PLLA-based samples, the changes of crystalline structures in cooling process were investigated with the in situ WAXD with hot stage. Figure 7 shows the diffraction intensity changes of PLLA/PDLA and LCBPLA/PDLA samples recorded upon a cooling program with various thermal treatment temperature ( $T_s = 190, 220$  and 230 °C). Based on these WAXD data, the intensity changes of  $S_c$  (110) diffraction and  $H_c$  (110)/(200) diffraction were evaluated, as depicted in Fig. 8. As shown in Fig. 7, when the melting temperature

exceeds 190 °C, all samples do not show any discernable diffraction peaks of  $H_c$ . During the cooling process, the diffraction peaks of  $H_c$  can be noticed at approximately 140 °C. The intensity of 110/200 plane for  $H_c$  crystallites increases gradually with the cooling temperature decreasing from 140 to 80 °C. However, the intensity of 110 plane for  $S_c$  crystallites has no clear changes. This phenomenon suggests that the  $S_c$  crystals could be retained when the melting temperature is lower than 220 °C. Moreover, in comparison with other samples at various melting temperature, the intensity is noted to be the strongest for the  $S_c$  crystals at the cooling temperature of 220 °C. When the temperature is higher than 220 °C, all the samples does not show any visible diffraction peaks, indicating that there are only the amorphous crystals before the cooling treatment as shown in Fig. 8c and f. However, with cooling down the sample from 230 °C, the diffraction peaks of  $S_c$  are observed when the temperature is approaching around 210 °C. As for the LCBPLA sample, the diffraction peak of  $S_c$  appears to be clearly noted and the peak area rapidly increases, as shown in Fig. 8f.

To have a deep insight into understanding these phenomena, we propose a speculated mechanism

**Figure 7** WAXD patterns of samples during cooling process, a–c: LCBPLA + 10% PDLA and d–f: PLLA + 10% PDLA.



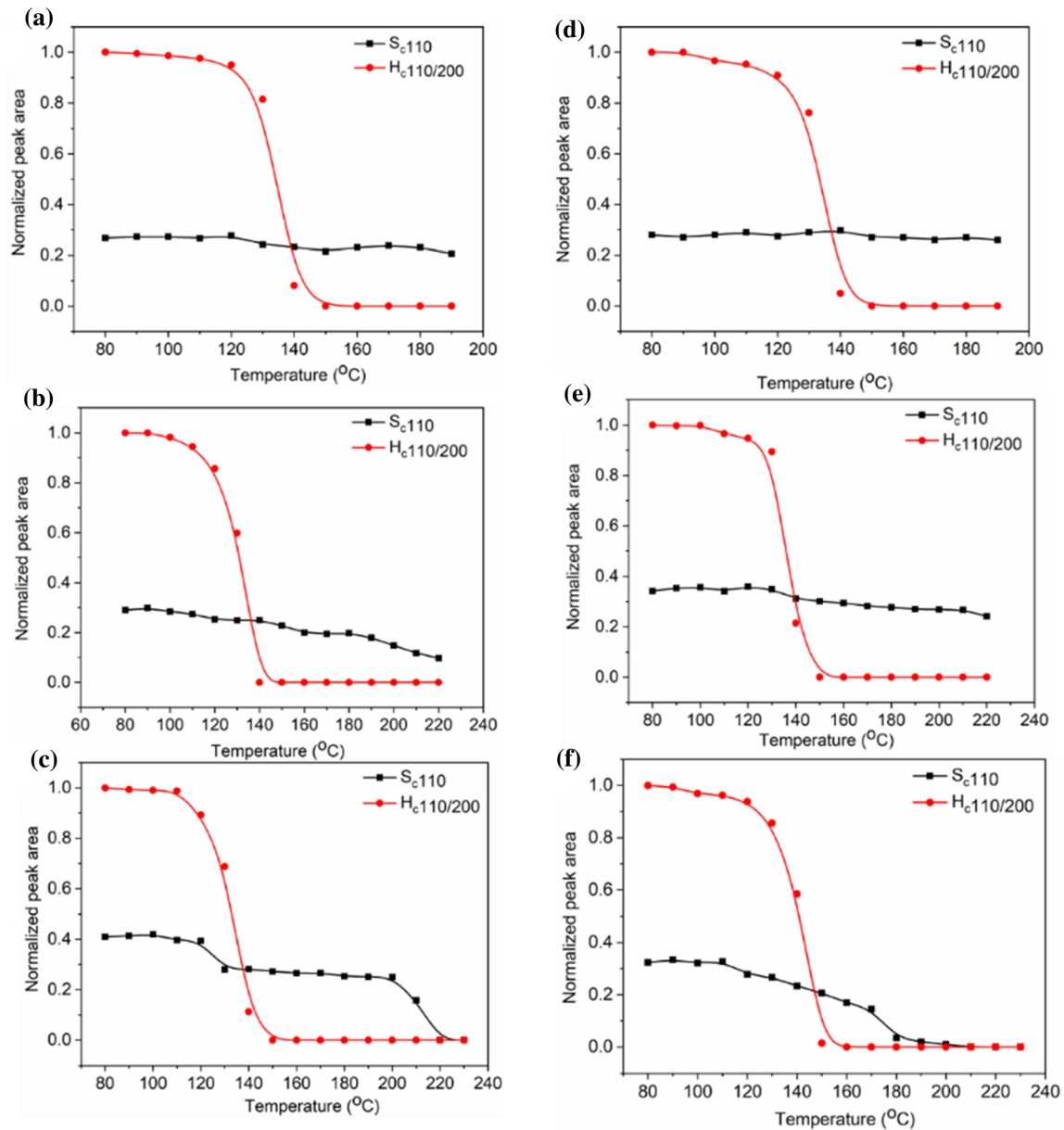


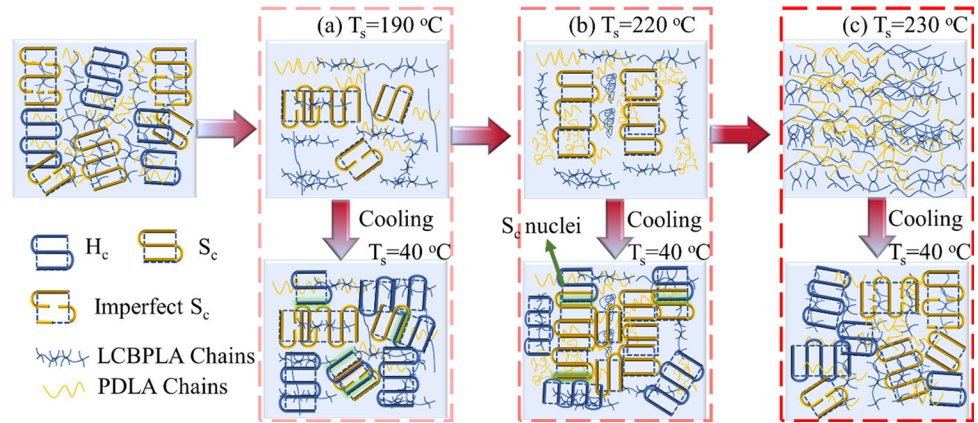
**Figure 8** Temperature-dependent peak areas for  $S_c$  (110) diffraction and  $H_c$  (110)/(200) diffraction upon heating the PLLA/PDLA and LCBPLA/PDLA blends. Peak area was normalized by the maximum value of  $H_c$  (110)/(200) diffraction

with aspect to changing the crystalline structure of  $S_c$  and various nucleation effectiveness upon thermal treatment temperature, as shown in Fig. 9. It is thought that when the melting temperature is lower than 190 °C (Fig. 9a), the  $S_c$  crystals on one hand tend to stay unmelted and embedded among the PLA molecular chains, which can act as nucleation sites during cooling stage. On the other hand, the unmelted  $S_c$  significantly improves the crystallization

of each sample. a–c: PLLA/PDLA and d–f: LCBPLA/PDLA. Black curves represent the results regarding  $S_c$  intensity while red curves for  $H_c$  intensity.

ability of polymer molecules to form  $H_c$  crystals. With increasing the melting temperature to 220 °C (lower than the melting temperature of  $S_c$ , Fig. 9b), some  $S_c$  crystals with less integrated structures would be melted and other unmelted  $S_c$  would promote the development of  $S_c$  itself and act as the heterogeneous nucleation sites for  $H_c$  during the cooling process, leading to the formation of the relatively perfect  $S_c$  crystals and thus a higher melt temperature (as

**Figure 9** Schematic illustration of the evolution of crystalline structures of the LCBPLA/PDLA sample with various thermal treatment temperatures ( $T_s$ ).



shown in Fig. 6b, d). When the thermal treatment temperature reaches to 230 °C (Fig. 9c), the  $S_c$  crystals would completely melt and PDLA molecules would well disperse in the polymer matrix. During the cooling process, the  $S_c$  crystals with small area size and less integrated structures will be reformed, inducing the crystallization behavior of the  $S_c$  and  $H_c$  crystals simultaneously. Consequently, the less integrated  $S_c$  crystals can act as the stereocomplex nucleating agents and thus enhance the melting temperature  $T_o$  of these blends. Above all, the  $S_c$  crystals appear to keep diverse configuration states due to the cooling treatments starting from different melting temperatures, thus producing different influences on the crystallization behavior of the PLA molecule. Specially, the crystallization ability is clearly enhanced when the blends are cooled from 230 °C at which the  $S_c$  can be fully melted, followed by the formation of the crystals with integrated structure.

### Nucleation enhancement by high melting point PLA crystallites

To study effect of  $S_c$  crystallites and molecular weight on the nucleation efficiency (NE), the self-nucleation experiment is presented in Fig. 10 and the NE term is also defined as follows with the crystallization temperature ( $T_p$ ) [40, 41]:

$$NE(\%) = \frac{T_p - T_p^{min}}{T_p^{max} - T_p^{min}} \times 100\% \quad (1)$$

where  $T_p^{min}$  is the crystallization peak temperature of pure polymer and  $T_p^{max}$  corresponds to the maximum crystallization temperature for a ‘self-nucleated’ melt. For the processed PLLA melt,  $T_p^{min}$  is determined to

be 99.4 °C, while  $T_p^{max}$  is determined to be 141.8 °C, which can be found in Fig. 10a. Because of the self-nucleation seeds created by the melting behavior in the partial melting zone, the crystallization peak temperature increased sharply with the decrease of  $T_s$  [38, 39]. According to the reports [30, 41],  $T_p^{max}$  should occur at the lowest  $T_s$  of the partial melting zone and can be obtained in Fig. 10. Figure 10b shows that  $T_s = 168$  °C is the lowest temperature, since the melting peak is only discerned when  $T_s$  is lower than 168 °C. Thus,  $T_p^{max} = 141.8$  °C is achieved.

Using the  $T_p$  obtained from the nonisothermal crystallization (Fig. 5), the nucleation efficiency is obtained in Fig. 11. The NE rapidly increases from 52.2% for PLLA + 10% PDLA sample to 95.9% for LCBPLA + 10%PDLA blend. This is because the long-chain branches can provide more nucleation sites and promote the formation of more  $S_c$ . The long-chain branches play an important role in forming nucleation sites, markedly enhancing the nucleation ability of PLLA during the cooling process, due to the branched topological structure. Hence, they can significantly enhance crystalline temperatures (onset and peak crystalline temperatures) and ability, facilitating the crystallization. However, as further increasing the content of PDLA (more than 5 wt% PDLA), the NE value slightly decreases from 98.3% to 96.2%, indicating that 5 wt% PDLA is an optimal addition for improving the NE value. Introducing the long-chain branches into PDLA blends can promote the development of  $S_c$ , inducing the enhancement of  $S_c$  content. During the cooling process, the  $S_c$  can act as the heterogeneous sites and improve the crystalline ability. However, the forming amount content of  $S_c$  can entangle the PLLA molecular chains and form the network, prohibiting the movements of the



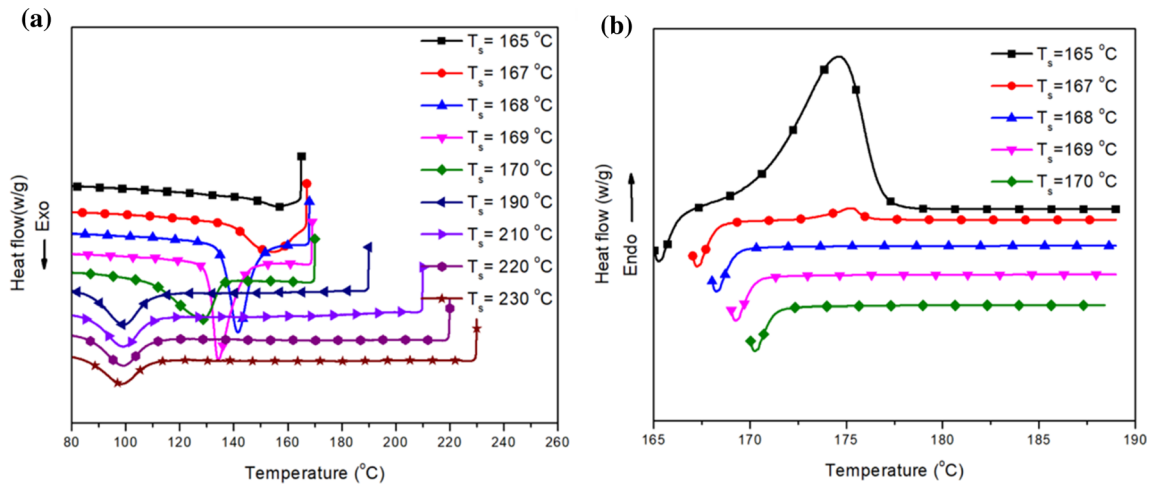


**Figure 10** The DSC cooling curves of PLLA at various thermal treatment temperatures **a** and the second-melting curves **b**.

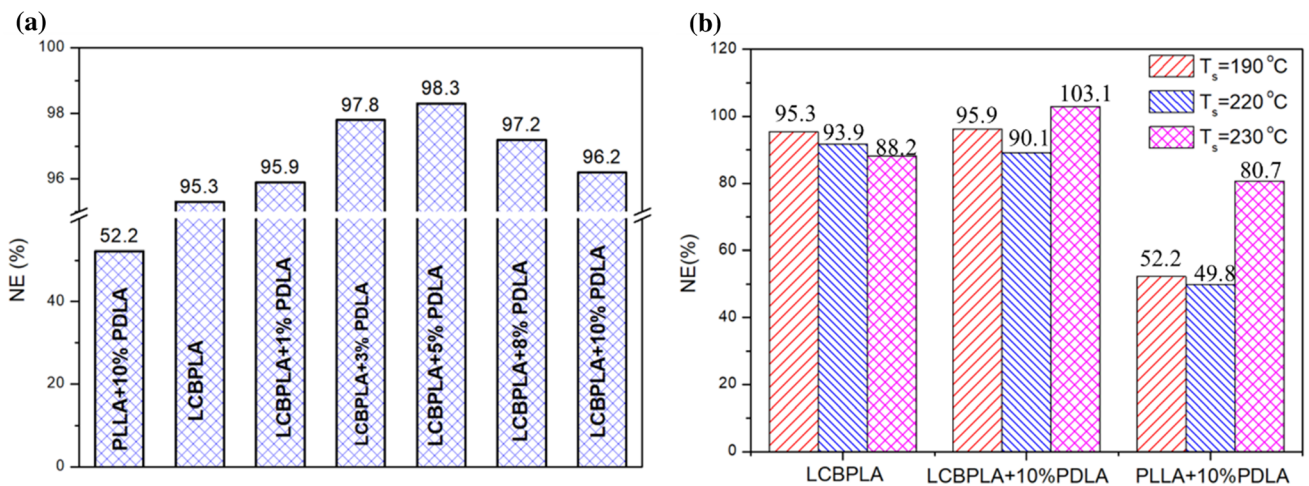


**Figure 11** **a** Nucleation efficiency (NE) of PLLA at various contents of PDLA at 190 °C and **b** Nucleation efficiency of PLLA at different thermal treatment temperatures.

molecular chains. It is expected that this prohibiting factor plays a dominant role when the PDLA content exceeds 5 wt%, resulting in the decrease of the crystalline temperatures, as shown in Fig. 5 and Table 3.

In addition, the effect caused by the annealed temperature on the NE value was also investigated. As shown in Fig. 11b, an expected phenomenon for LCBPLA melt is observed that the NE value decreases gradually with increasing the  $T_s$  temperature from 190 to 230 °C. However, an opposite phenomenon for the LCBPLA or PLLA blend with 10% PDLA melt is noted that NE value decreases slightly from 190 to 220 °C firstly but then increases significantly with further increasing  $T_s$  to 230 °C. The reason could be due to the varying melting behavior of  $S_c$  crystals in blend with adding PDLA, thus resulting

in different crystallization behavior during cooling process from the desired  $T_s$  (190, 220 or 230 °C). The possible explanations are presented as follows: increasing the melt temperature from 190 °C to 220 °C can promote the melting of some parts of the pre-existed imperfect  $S_c$  crystals due to the  $S_c$  with a melting temperature of 225 °C. It means that as the melt is cooled from the  $T_s$  of 220 °C, the reserved  $S_c$  crystals can work as the temperate for forming the new  $S_c$  and optimizing the incomplete  $S_c$  thus having a larger crystal thickness and size, which as a result enhances the crystalline temperature of  $S_c$ , as shown in Fig. 6. [42] Hence, the resulting relatively perfect  $S_c$  in case of  $T_s = 220\text{ }^\circ\text{C}$  in comparison with the incomplete  $S_c$  at  $T_s = 190\text{ }^\circ\text{C}$  could perform a larger ability of the heterogeneous nucleation for  $H_c$

crystals. However, it can also be expected that the complex network between  $S_c$  and PLLA molecular chains can be built with  $T_s = 220$  °C, resulting from forming perfect  $S_c$  among molecular chains. In this case, the molecular chains can be entangled and the mobility of PLLA molecules is decreased, thus weakening the heterogeneous nucleation ability in comparison to the case at  $T_s = 190$  °C. The two factors seem to play an opposite role in influencing the NE value. Therefore, a slight decrease of NE value is observed for both LCBPLA and PLLA blend by increasing  $T_s$  from 190 to 220 °C, shown in Fig. 11. With the  $T_s$  temperature at 230 °C, in the cooling process, driven by a large supercooling, the chain bundles or crystals fragments can form complete  $S_c$  crystals with relatively more smooth and larger surfaces compared with the corresponding samples treated at 220 °C, which is able to act as new templates for the further formation of smaller complete  $S_c$ , as illustrated in Fig. 9c. Simultaneously, the inhibiting effect of network to the movement of PLLA molecular chains becomes weak due to a weaker suppression effect from network structures formed by  $S_c$  and PLLA molecules. Both two factors play a role in providing sufficient nucleating site and templates effect to promote the improvement of  $H_c$  crystalline ability as compared to that with  $T_s = 220$  °C, leading to the crystalline temperature significantly enhanced (as shown in Fig. 6) and a large enhancement of NE value (seen in Fig. 11b).

### Crystalline morphology during isothermal crystallization process

To demonstrate the effect of long-chain branched structures on the spherulitic growth of  $S_c$  crystallites, isothermal crystallization behavior was investigated by means of the POM characterization, as shown in Fig. 12 and Table 4. The isothermal temperature was set at 156 °C, at which the formation of  $H_c$  was not able to occur so that only the  $S_c$  existed. The POM micrographs of LCBPLA/PDLA with various PDLA content are displayed in Fig. 12. As expected, introducing PDLA appears to induce the formation of much more crystallization sites at the beginning of the crystallization process. Increasing the PDLA content enlarges the number of these  $S_c$  spherulites from 80 to 109 and the size from 56.47 to 94.13  $\mu\text{m}$ . Furthermore, with increasing the PDLA content, there needs a shorter time for an instant observation

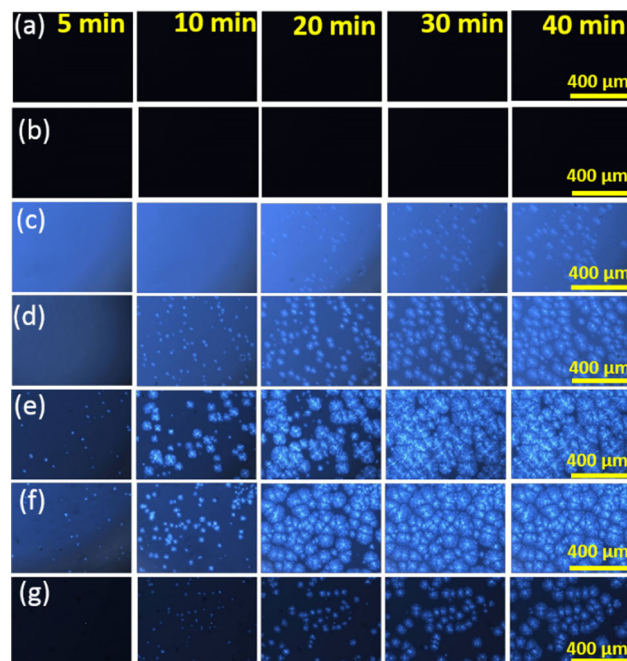


**Figure 12** Selected POM micrographs during isothermal crystallization at  $T_s$  of 156 °C for the samples of **a** LCBPLA, **b** LCBPLA + 1%PDLA, **c** LCBPLA + 3%PDLA, **d** LCBPLA + 5%PDLA, **e** LCBPLA + 8%PDLA, **f** LCBPLA + 10%PDLA and **g** PLLA + 10%PDLA.

**Table 4** Numbers of Nuclei counted for neat PLLA and LCBPLA/PDLA blends with various PDLA concentrations at temperature = 156 °C

Sample	(a)	(b)	(c)	(d)	(e)	(f)	(g)
Number	0	0	80	109	94	89	72
Average size ( $\mu\text{m}$ )	0	0	56.47	69.7	86.7	94.13	78.4

for the appearance of the spherulites. As a consequence, the combined effect of increasing crystallization time and PDLA content contributes to a larger density and size of spherulites. In addition, as shown in Fig. 12f, g, there are spherulites with larger size and nucleation density for the LCBPLA + 10% PDLA blends as compared with liner PLLA + 10% PDLA blends, indicating that the long-chain branches allow for accelerating the growing rate of  $S_c$  crystallites. We attribute this to the factor as follows: when the melt was cooled from 230 °C, the long-chain branches can provide more branched structures acting as heterogeneous nucleation sites, so with introducing the long-chain branches, more  $S_c$  were formed (as shown in Table 4), thus, providing more

nucleation sites or surface. With more heterogeneous nucleation sites, the overall crystallization rate of  $S_c$  should be further increased, so that the nucleation density was further enhanced. Back to Fig. 6, it is seen that the  $S_c$  can be completely melted when the cooling process starts from a temperature high to 230 °C, which leads to the release of the PDLA molecular chains. Consequently, it explains the reason why the formation of  $S_c$  crystals occurs firstly during the whole crystallization process.

## Conclusions

In summary, an effective approach is proposed to enhance the  $S_c$  crystallization ability but depress the homocrystallization of PLLA molecule regarding the PLLA/PDLA blends by the miscible polymer blending with hydrogen bond interactions. The formation of  $S_c$  can significantly improve the rheological properties including the  $G'$  and  $G''$  of melt due to the cross-linking network configurations composed of the  $S_c$  and long-chain branches. Provided certain processing conditions,  $S_c$  are exclusively formed in both nonisothermal and isothermal crystallizations of LCBPLA/PDLA blend. Homocrystallization is dramatically suppressed and the crystallization behavior of the  $S_c$  crystals becomes predominant by means of introducing long-chain branches to the linear PLLA molecules and increasing the PDLA content. The long-chain branches are able to significantly increase the crystalline ability of  $S_c$  crystals from 20.1% (PLLA + 10%PDLA)–30.4% (LCBPLA + 10%PDLA) and enlarge the average size of spherulites from 78.4 to 94.13  $\mu\text{m}$ . Furthermore the combined effect of PDLA and long-chain branches sharply enhances the nucleation density from 52.2% for PLLA + 10% PDLA–98.3% for LCBPLA + 5%PDLA and reach the highest nucleation promoting effect. During melting process, changing the thermal treatment temperatures can make  $S_c$  with diverse topological configuration structures. Increasing the melting temperature from 190 to 230 °C can promote the development of  $S_c$  with more integrated structures. During the cooling stage, the presence of  $S_c$  crystals moves the crystallization temperature to a higher value. Our work will provide a guidance for a new design strategy for new PLA-based materials and using  $S_c$  as a nucleation agent in actual industrial applications.

## Acknowledgement

This paper was funded by Fund of Education Department of Shaanxi Province (20JK0564), Talent Launch Project of Shaanxi University of Technology (SLGRCQ2001) and China Postdoctoral Science Foundation (2020M673585XB). We are indebted to Shanghai Synchrotron Radiation Facility (SSRF) for providing WAXD measurements.

## Compliance with ethical standards

**Conflict of interest** The authors declare that there is no conflict of interest.

## References

- [1] Jin Z, Yin HM, Hsiao BS, Zhong GJ, Li ZM (2014) Biodegradable Poly(lactic Acid)/Hydroxyl Apatite 3d Porous Scaffolds using high-pressure molding and salt leaching. *J Mater Sci* 49:1648–1658. <https://doi.org/10.1007/s10853-013-7848-x>
- [2] Zhao ZG, Yang Q, Coates PD, Whiteside B, Kelly AL, Huang Y, Wu PP (2018) Structure and property of microinjection moulded Poly (lactic Acid) with high degree of long chain branching. *Ind Eng Chem Res* 57:11312–11322. <https://doi.org/10.1021/acs.iecr.8b01597>
- [3] Wang Y, Lei M, Wei Q, Wang Y, Zhang J, Guo Y, Saroia J (2020) 3D printing biocompatible L-Arg/Gnps/PLA nanocomposites with enhanced mechanical property and thermal stability. *J Mater Sci* 55:5064–5078. <https://doi.org/10.1007/s10853-020-04353-8>
- [4] Wang L, Jing X, Cheng H, Hu X, Yang L, Huang Y (2012) Rheology and crystallization of long-chain branched poly (L-Lactide) S with controlled branch length. *Ind Eng Chem Res* 51:10731–10741. <https://doi.org/10.1021/ie300524j>
- [5] Hu W, Zhang Y, Qi Y, Wang H, Liu B, Zhao Q, Zhang J, Duan J, Zhang L, Sun Z, Liu B (2020) Improved mechanical properties and flame retardancy of wood/pla all-degradable biocomposites with novel lignin-based flame retardant and tgc. *Macro Mater Eng* 305:1900840. <https://doi.org/10.1002/mame.201900840>
- [6] Liu J, Lou L, Yu W, Liao R, Li R, Zhou C (2010) Long chain branching polylactide: structures and properties. *Polymer* 51:5186–5197. <https://doi.org/10.1016/j.polymer.2010.09.002>
- [7] Li Z, Zhao X, Lin Y, Coates P, Caton-Rose F, Martyn M (2015) Structure and blood compatibility of highly oriented poly( L-lactic acid) chain extended by Ethylene Glycol

- Diglycidyl Ether. *Polymer* 56:523–534. <https://doi.org/10.1016/j.polymer.2014.11.035>
- [8] Hirata M, Kimura Y (2008) Thermomechanical properties of stereoblock Poly (lactic acid) s with different PLLA/PDLA block compositions. *Polymer* 49:2656–2661. <https://doi.org/10.1016/j.polymer.2008.04.014>
- [9] He Y, Xu Y, Wei J, Fan Z, Li S (2008) Unique crystallization behavior of Poly (L-Lactide)/Poly (D-Lactide) stereocomplex depending on initial melt states. *Polymer* 49:5670–5675. <https://doi.org/10.1016/j.polymer.2008.10.028>
- [10] Sarasua J, Arraiza AL, Balerdi P, Maiza I (2005) Crystallization and thermal behaviour of optically pure Polylactides and their blends. *J Mater Sci* 40:1855–1862. <https://doi.org/10.1007/s10853-005-1204-8>
- [11] Tsuji H, Horii F, Hyon SH, Ikada Y (1991) Stereocomplex formation between Enantiomeric Poly (Lactic Acid) S. 2 stereocomplex formation in concentrated solutions. *Macromolecules* 24:2719–2724. <https://doi.org/10.1021/ma00010a013>
- [12] Tsuji H, Hyon SH, Ikada Y (1992) Stereocomplex formation between Enantiomeric Poly (Lactic Acids). 5. calorimetric and morphological studies on the stereocomplex formed in Acetonitrile Solution. *Macromolecules* 25:2940–2946. <https://doi.org/10.1021/ma00037a024>
- [13] Tsuji H, Ikada Y (1996) Crystallization from the melt of Poly (Lactide) S with different optical purities and their blends. *Macro Chem Phy* 197:3483–3499. <https://doi.org/10.1002/macp.1996.021971033>
- [14] Purnama P, Jung Y, Kim SH (2012) Stereocomplexation of Poly(L-Lactide) and random copolymer Poly(D-Lactide-Co-E-Caprolactone) to enhance melt stability. *Macromolecules* 45:4012–4014. <https://doi.org/10.1021/ma202814c>
- [15] Biela T, Duda A, Penczek S (2006) Enhanced melt stability of star-shaped stereocomplexes as compared with linear stereocomplexes. *Macromolecules* 39:3710–3713. <https://doi.org/10.1021/ma060264r>
- [16] Bao RY, Yang W, Wei XF, Xie BH, Yang MB (2014) Enhanced formation of stereocomplex crystallites of high molecular weight poly (L-Lactide)/poly (D-Lactide) blends from melt by using poly (Ethylene Glycol). *ACS Sustain Chem Eng* 2:2301–2309. <https://doi.org/10.1021/sc500464c>
- [17] Tsuji H, Sugimoto S (2015) Accelerated stereocomplex crystallization of poly(L-Lactide)/poly(D-Lactide) blends by long terminal linear alkyl groups. *Macro Mater Eng* 300:391–402. <https://doi.org/10.1002/mame.201400401>
- [18] Pan P, Han L, Bao J, Xie Q, Shan G, Bao Y (2015) Competitive stereocomplexation, homocrystallization, and polymorphic crystalline transition in poly (L-Lactic Acid)/poly (D-Lactic acid) racemic blends: molecular weight effects. *J Phy Chem B* 119:6462–6470. <https://doi.org/10.1021/acs.jpcc.5b03546>
- [19] Han L, Pan P, Shan G, Bao Y (2015) Stereocomplex crystallization of high-molecular-weight Poly (L-Lactic Acid)/Poly (D-Lactic Acid) racemic blends promoted by a selective nucleator. *Polymer* 63:144–153. <https://doi.org/10.1016/j.polymer.2015.02.053>
- [20] Brochu S, Prud'Homme RE, Barakat I, Jerome R (1995) Stereocomplexation and morphology of polylactides. *Macromolecules* 28:5230–5239. <https://doi.org/10.1021/ma00119a010>
- [21] Bao RY, Yang W, Jiang WR, Liu ZY, Xie BH, Yang MB, Fu Q (2012) Stereocomplex formation of high-molecular-weight Polylactide: a low temperature approach. *Polymer* 53:5449–5454. <https://doi.org/10.1016/j.polymer.2012.09.043>
- [22] Bao RY, Yang W, Jiang WR, Liu ZY, Xie BH, Yang MB (2013) Polymorphism of Racemic Poly(L-Lactide)/Poly(D-Lactide) blend: effect of melt and cold crystallization. *J Phy Chem B* 117:3667–3674. <https://doi.org/10.1021/jp311878f>
- [23] Badrinarayanan P, Dowdy KB, Kessler MR (2010) A Comparison of crystallization behavior for melt and cold crystallized Poly (-Lactide) using rapid scanning rate calorimetry. *Polymer* 51:4611–4618. <https://doi.org/10.1016/j.polymer.2010.08.014>
- [24] Wasanasuk K, Tashiro K (2011) Structural regularization in the crystallization process from the glass or melt of Poly(L-Lactic Acid) viewed from the temperature-dependent and time-resolved measurements of Ftir and wide-angle/small-angle x-ray scatterings. *Macromolecules* 44:9650–9660. <https://doi.org/10.1021/ma2017666>
- [25] Bing N, Tian N, Lv R, Li Z, Xu W, Qiang F (2010) Evidence of sequential ordering during cold crystallization of Poly (-Lactide). *Polymer* 51:563–567. <https://doi.org/10.1016/j.polymer.2009.11.064>
- [26] Vasanthan N, Ly H, Ghosh S (2011) Impact of nanoclay on isothermal cold crystallization kinetics and polymorphism of Poly(L-Lactic Acid) nanocomposites. *J Phy ChemB* 115:9556. <https://doi.org/10.1021/jp203322d>
- [27] Cartier L, Okihara T, Lotz B (1997) Triangular polymer single crystals: stereocomplexes, twins, and frustrated structures. *Macromolecules* 30:6313–6322. <https://doi.org/10.1021/ma9707998>
- [28] Rahman N, Kawai T, Matsuba G, Nishida K, Kanaya T, Watanabe H, Okamoto H, Kato M, Usuki A, Matsuda M (2009) Effect of Polylactide Stereocomplex on the crystallization behavior of Poly(L-lactic acid). *Macromolecules* 42:4739–4745. <https://doi.org/10.1021/ma900004d>
- [29] Zhou KY, Li JB, Wang HX, Wang JR (2017) Effect of star-shaped chain architectures on the polylactide stereocomplex



- crystallization behaviors. *C J Polym Sci* 35:974–991. <https://doi.org/10.1007/s10118-017-1935-4>
- [30] Wei XF, Bao RY, Cao ZQ, Yang W, Xie BH, Yang MB (2012) Stereocomplex crystallite network in asymmetric PLLa/Pdla blends: formation, structure, and confining effect on the crystallization rate of homocrystallites. *Macromolecules* 47:1439–1448. <https://doi.org/10.1021/ma402653a>
- [31] Du F, Scogna RC, Zhou W, Brand S, Fischer JE, Winey KI (2004) Nanotube networks in polymer nanocomposites: rheology and electrical conductivity. *Macromolecules* 37:9048–9055. <https://doi.org/10.1021/ma049164g>
- [32] Xu Z, Niu Y, Wang Z, Li H, Yang L, Qiu J, Wang H (2011) Enhanced nucleation rate of polylactide in composites assisted by surface acid oxidized carbon nanotubes of different aspect ratios. *ACS Appl Mater Inter* 3:3744–3753
- [33] Xu Z, Niu Y, Yang L, Xie W, Li H, Gan Z, Wang Z (2010) Morphology, rheology and crystallization behavior of polylactide composites prepared through addition of five-armed star polylactide grafted multiwalled carbon nanotubes. *Polymer* 51:730–737. <https://doi.org/10.1016/j.polymer.2009.12.017>
- [34] Liu C, Zhang J, He J, Hu G (2003) Gelation in carbon nanotube/polymer composites. *Polymer* 44:7529–7532. <https://doi.org/10.1016/j.polymer.2003.09.013>
- [35] Horst RH, Winter HH (2000) Stable critical gels of a copolymer of Ethene and 1-Butene achieved by partial melting and recrystallization. *Macromolecules* 33:7538–7543. <https://doi.org/10.1021/ma000361z>
- [36] Huang S, Liu Z, Yin C, Gao Y, Wang Y, Yang M (2012) Gelation of Attractive Particles in Polymer Melt. *Polymer* 53:4293–4299. <https://doi.org/10.1016/j.polymer.2012.07.054>
- [37] Hu W, Frenkel D, Mathot VB (2003) Intramolecular nucleation model for polymer crystallization. *Macromolecules* 36:8178–8183. <https://doi.org/10.1021/ma0344285>
- [38] Liu Z, Chen Y, Ding W, Zhang C (2015) Filling behavior, morphology evolution and crystallization behavior of microinjection molded poly (Lactic Acid)/Hydroxyapatite nanocomposites. *Compos Part A-Appl Science Manuf* 72:85–95. <https://doi.org/10.1016/j.compositesa.2015.02.002>
- [39] Yamane H, Sasai K (2003) Effect of the addition of poly (D-Lactic Acid) on the thermal property of poly (L-Lactic Acid). *Polymer* 44:2569–2575. [https://doi.org/10.1016/S0032-3861\(03\)00092-2](https://doi.org/10.1016/S0032-3861(03)00092-2)
- [40] Fillon B, Thierry A, Lotz B, Wittmann J (1994) Efficiency scale for polymer nucleating agents. *J Therm Anal* 42:721–731. <https://doi.org/10.1007/BF02546745>
- [41] Fillon B, Wittmann J, Lotz B, Thierry A (1993) Self-nucleation and recrystallization of isotactic polypropylene ( $\alpha$  phase) investigated by differential scanning calorimetry. *J Polym Sci Part B Polym Phys* 31:1383–1393. <https://doi.org/10.1002/polb.1993.090311013>
- [42] Wu PP, Yang Q, Zhao ZZ, Zhang TY, Huang YJ, Liao X (2018) Realizing simultaneous toughening and reinforcement in polypropylene blends via solid die-drawing. *Polymer* 161:109–121. <https://doi.org/10.1016/j.polymer.2018.12.011>

**Publisher's Note** Springer Nature remains neutral with regard to jurisdictional claims in published maps and institutional affiliations.